First Isolation of Monomeric *N*-Alkoxyarylaminyl Radicals and Their Chemical and Magnetic Properties[1]

Yozo Miura,* Tatsuya Tomimura, Nobuaki Matsuba, Rika Tanaka, and Masaaki Nakatsuji

Department of Applied Chemistry, Graduate School of Engineering, Osaka City University, Sumiyoshi-ku, Osaka 558-8585, Japan

Yoshio Teki

Department of Material Science, Graduate School of Science, Osaka City University, Sumiyoshi-ku, Osaka 558-8585, Japan

miura@a-chem.eng.osaka-cu.ac.jp

Received June 19, 2001

The present report describes the first isolation of monomeric *N*-alkoxyarylaminyls and their chemical and magnetic properties. Reaction of the corresponding lithium amides of 2,4-diaryl-6-*tert*-butylanilines, 2,6-diaryl-4-*tert*-butylanilines, or 2,4,6-triarylanilines with *tert*-butyl peroxybenzoate in THF at −78 °C yielded quite persistent *N*-*tert*-butoxy-2,4-diaryl-6-*tert*-butylphenylaminyls (**1**), *N*-*tert*-butoxy-2,6-diaryl-4-*tert*-butylphenylaminyls (**2**), and *N*-*tert*-butoxy-2,4,6-triarylphenylaminyls (**3**), respectively, which were isolated in the monomeric form in 17−25% yields. All radicals prepared were oxygen insensitive and thermally very stable. X-ray crystallographic analyses were carried out for two radicals, and it was shown that the N and O atoms are coplanar with the anilino benzene ring. The ESR spectra of **1**−**3** gave $a_N = 0.984-1.05$ and a_H (anilino meta) = 0.158−0.170 mT (g = 2.0041−2.0043), indicating that the unpaired electron mainly resides on the nitrogen and anilino benzene ring. Magnetic susceptibility measurements for **1** and **3** showed that one radical revealed a weak ferromagnetic interaction and an analysis by the Curie−Weiss law gave 0.3 K as θ. The other radicals examined showed weak antiferromagnetic interactions and θ's were determined to be −0.3 to −1.5 K.

Introduction

Although a variety of *N*-alkoxyalkylaminyls (RṄOR),[2−11] *N*-alkoxyvinylaminyls,[6] and *N*-alkoxyarylaminyls (ArṄOR)[2−4,6−10] have widely been investigated by ESR spectroscopy over a long period and some persistent *N*-alkoxyaminyls have been found, there have been no reports of isolation of *N*-alkoxyaminyls. This is in contrast to the chemistry of isoelectronic thioaminyl radicals (RṄSR).[12,13] Since the first ESR studies on *N*-(phenylthio)phenylaminyl (PhṄSPh) were independently reported by two groups,[14] a number of studies on thioaminyls have been carried out and their electronic structures, stabilities (lifetimes), and decomposition mechanism have widely been elucidated. On the basis of the large body of accumulated data, possible isolable thioaminyls have been designed, and effort has been paid to their preparation and isolation. Although *N*-[(4-nitrophenyl)thio]-2,4,6-tri-*tert*-butylphenylaminyl was the first isolated thioaminyl,[15] this radical was immediately decomposed by the reaction with atmospheric oxygen. In the continuing studies, we have found a variety of oxygen-insensitive and isolable stable thioaminyl radicals; typical examples are *N*-(arylthio)-2,4,6-triarylphenylaminyls[16] and *N*-(arylthio)-2-*tert*-butyl or *N*-(arylthio)-2,7-di-*tert*-butyl-1-pyrenylaminyl radicals.[17] Although free radical chemistry has been developed over a long time, isolable stable free radicals are still rare.[18] In recent years, such oxygen-insensitive and isolable stable free radicals have at-

* To whom correspondence should be addressed. Fax: +81-6-6605-2769.

(1) ESR Studies of Nitrogen-Centered Free Radicals. 54. For part 53, see: Nakatsuji, M.; Miura, Y.; Teki, Y. *J. Chem. Soc., Perkin Trans. 2* **2001**, 738.

(2) Danen, W. C.; Neugebauer, F. A., *Angew. Chem., Int. Ed. Engl.* **1975**, *14*, 783.

(3) Danen, W. C.; West, C. T.; Kensler, T. T. *J. Am. Chem. Soc.* **1973**, *95*, 5716.

(4) Kaba, R. A.; Ingold, K. U. *J. Am. Chem. Soc.* **1976**, *98*, 7375.

(5) Woynar, H.; Ingold, K. U. *J. Am. Chem. Soc.* **1980**, *102*, 3813.

(6) Ahrens, W.; Wieser, K.; Berndt, A. *Tetrahedron Lett.* **1973**, 3141.

(7) Balaban, A. T.; Frangopol, P. T.; Frangopol, M.; Negoitå, N. *Tetrahedron* **1967**, *23*, 4661.

(8) Terabe, S.; Konaka, R. *J. Chem. Soc., Perkin Trans. 2* **1973**, 369.

(9) Negoita, N.; Baican, R.; Balaban, A. T. *Tetrahedron Lett.* **1973**, 1877.

(10) Ahrens, W.; Berndt, A, *Tetrahedron Lett.* **1973**, 4281

(11) Negareche, M.; Boyer, M.; Tordo, P. *Tetrahedron Lett.* **1981**, *22*, 2879.

(12) Miura, Y. *Trends Org. Chem.* **1997**, *6*, 197−217.

(13) Miura, Y. *Recent Res. Dev. Org. Chem.* **1998**, *2*, 251−268.

(14) (a) Miura, Y.; Kinoshita, M. *Bull. Chem. Soc. Jpn.* **1977**, *50*, 1142. (b) Sayo, H.; Mori, K. *Chem. Pharm. Bull.* **1977**, *25*, 1489.

(15) Miura, Y.; Yamamoto, A.; Katsura, Y.; Kinoshita, M.; Sato, S.; Tamura, C. *J. Org. Chem.* **1982**, *47*, 2618.

(16) Miura, Y.; Tanaka, A.; Hirotsu, K. *J. Org. Chem.* **1991**, *56*, 6638.

(17) Miura, Y.; Yamano, E.; Tanaka, A.; Ymauchi, J. *J. Org. Chem.* **1994**, *59*, 3294.

(18) (a) Forrester, A. R.; Hay, J. M.; Thomson, R. H. *Organic Chemistry of Stable Free Radicals*; Academic Press: London and New York, 1968. (b) Rozantsev, E. G. *Free Nitroxyl Radicals*; Plenum Press: New York and London, 1970. (c) Volodarsky, L. B.; Reznikov, V. A.; Ovcharenko, V. I. *Synthetic Chemistry of Stable Nitroxides*; CRC Press: Boca Raton, FL, 1994.

10.1021/jo0106288 CCC: $20.00
Published on Web 10/04/2001

Chart 1

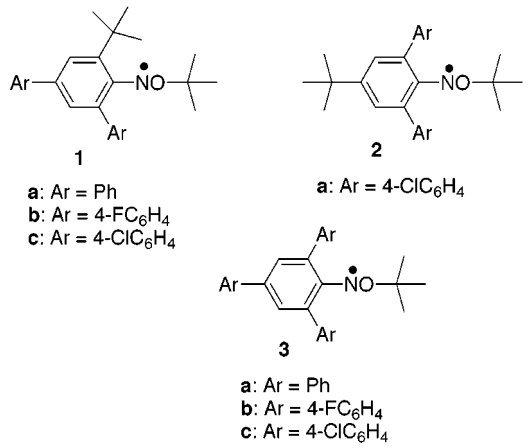

tracted much attention as a building block or magnetic spin source in the studies of organic magnetic materials.[19]

The purpose of the present study is to prepare sufficiently persistent *N*-alkoxyarylaminyls to be isolated. The basic strategy to accomplish this purpose is the complete protection of radicals from homolytic attacks by which the radicals are destroyed. Based on the knowledge accumulated in the studies of thioaminyl radicals, three kinds of *N*-alkoxyarylaminyls, **1**−**3**, were designed and prepared (Chart 1). In this paper we wish to report the first isolation of alkoxylarylaminyls and their chemical and magnetic properties.[20]

Results and Discussion

Generation of Alkoxyarylaminyl Radicals 1−3 and Their Isolation. There are a few methods for generation of *N*-alkoxyalkyl- and *N*-alkoyarylaminyls. The most convenient and widely applicable method is hydrogen-abstraction from the corresponding *N*-alkoxyalkyl- or *N*-alkoxyarylamines. Preparation of *N*-alkoxyalkylamines was already reported by Meesters and Benn.[21] This method, however, is limited to preparation of *N*-*tert*-butoxy-*tert*-alkylamines. Using the method, we tried to prepare *N*-*tert*-butoxy-2,4-diphenyl-6-*tert*-butylaniline (**4**) by the reaction of lithium 2,4-diphenyl-6-*tert*-butylphenylamide with *tert*-butyl peroxybenzoate (**5**) (Scheme 1). When a THF solution of 1 equiv of **5** was added to a solution of the lithium 2,4-diphenyl-6-*tert*-butylphenylamide, the resulting mixture immediately turned red, and TLC analysis showed formation of two red colored products, along with the presence of the unreacted starting aniline and formation of some minor products. The red colored products were isolated by column chromatography and identified on the basis of ^{1}H NMR, IR, and ESR spectra and elemental analyses. One of the red products was identified as 2,2′,4,4′-tetraphenyl-6,6′-di-*tert*-butylazobenzene (**6**) (yield 0.76%) on the basis of ^{1}H NMR and IR spectra and elemental analysis, and the other was identified as **1a** on the basis of IR and ESR spectra and elemental analysis (yield 11%). When separated by column chromatography, **1a** was a red oil but soon solidified to a red solid mass on standing. Recrystallization from MeOH gave red needles. Figure 1 shows an ESR spectrum of **1a** which consists of a 1:1:1 triplet. The IR spectrum showed no peak due to ν NH. The elemental analyses provided satisfactory agreements with the calculations as **1a**. Furthermore, its structure was later confirmed by an X-ray crystallographic analysis.

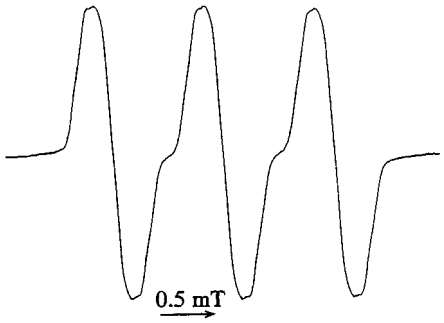

Figure 1. ESR spectrum of **1a** in benzene at 20 °C.

Scheme 1

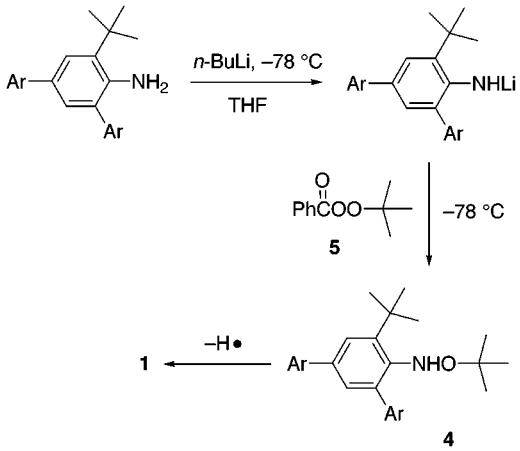

To improve the yields, the experimental conditions were examined. When two equiv of **5** for the lithium amide was employed, formation of **6** was not observed and the yield of **1a** was increased from 11 to 24%. However, an additional excess of **5** did not increase the yield. In the same manner, **1b** and **1c** were prepared and obtained as red needles in 20 and 17% yields, respectively.

This method was further applied for preparation of **2** and **3**. The reaction of lithium 2,6-bis(4-chlorophenyl)-4-*tert*-butylphenylamide with 2 equiv of **5** gave **2** in 20% yield, and the reaction of 2,4,6-triarylphenylamides with 2 equiv of **5** yielded **3a**−**c** in 17−18% yields. While **2**, **3b**, and **3c** were obtained as red or orange crystals, **3a** was a viscous oil. The spin concentration of the red oil determined by ESR was 92%.

A plausible mechanism for formation of **1**−**3** is described in Scheme 2. Previously, Meesters et al. proposed the mechanism for formation of *N*-*tert*-butoxy-*tert*-alkylamines from the reaction of lithium *tert*-alkylamides with **5**.[21] According to this mechanism, the reaction of **7** with **5** yields ketyl radical anion **8** and arylaminyl radical. The formed ketyl radical anion decomposes to lithium benzoate and *tert*-butoxyl radical. Coupling reaction between arylaminyl and *tert*-butoxyl radicals affords **9** (eqs 1−3). Equation 4 represents a homolytic attack of

(19) (a) *Magnetic Properties of Orgnaic Materials*; Lahti, P. M., Ed.; Marcel Dekker: New York and Basel, 1999, (b) Proceedings of the 6th International Conference on Molecule Based Magnets; Kahn, O., Ed.; *Mol. Cryst. Liq. Cryst.* **1999**, *334*, 1−712; *335*, 1−706.

(20) Part of this work was reported as a preliminary communication. see: Miura, Y.; Tomimura, T. *Chem. Commun.* **2001**, 627.

(21) Meesters, A. C. M.; Benn, M. H. *Synthesis* **1978**, 679.

Scheme 2

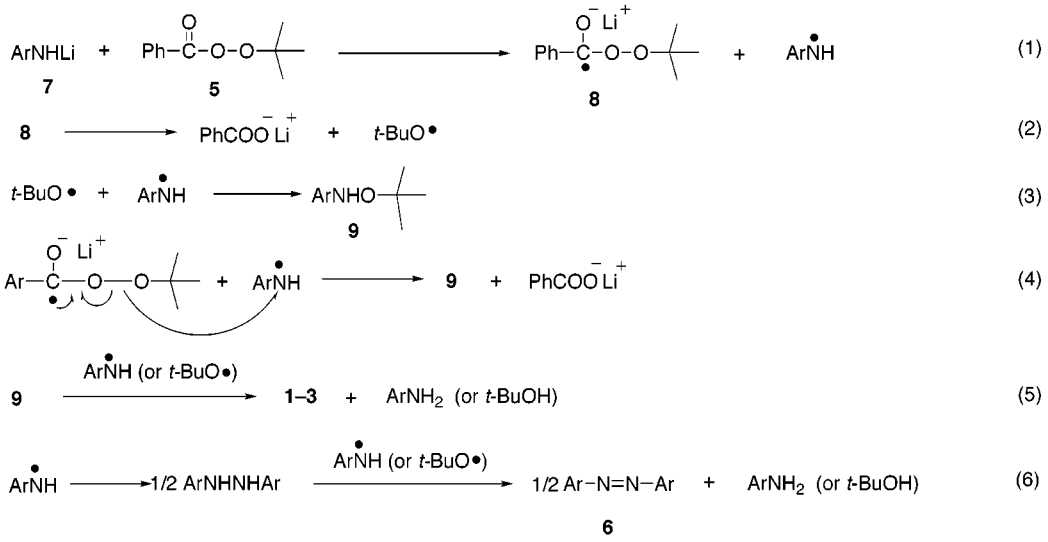

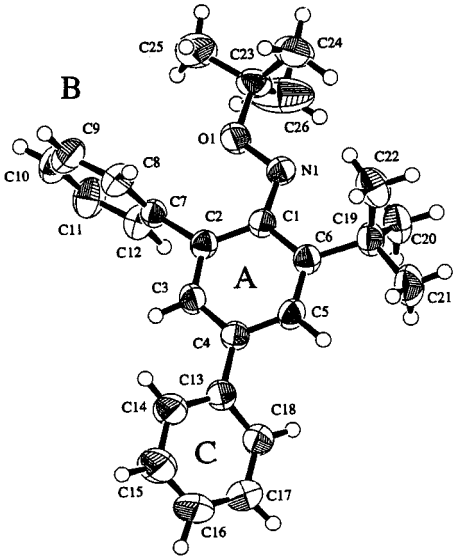

Figure 2. ORTEP drawing of **1a**. Selected bond lengths and angles and torsion angles are as follows: C1−N1 1.368(3), N1−O1 1.358(2), O1−C23 1.468(3), C1−C2 1.435(3), C1−C6 1.446-(3) Å; C1−N1−O1 111.1(2), N1−O1−C23 113.1(2)°; O1−N1−C1−C2 6.8(3), O1−N1−C1−C6 −175.4(2), C1−N1−O1−C23 −173.9(2)°.

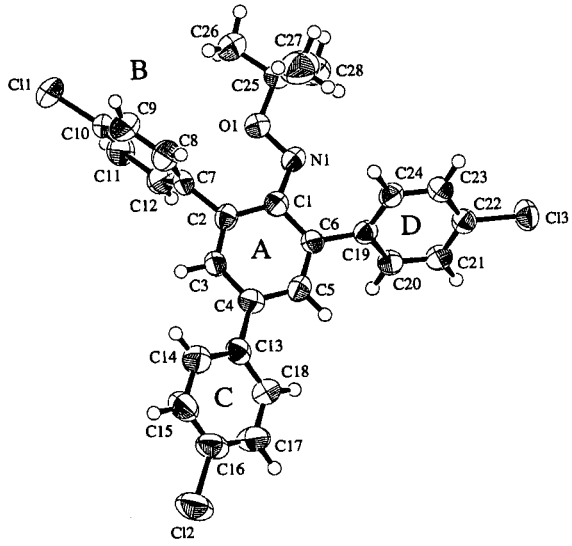

Figure 3. ORTEP drawing of **3c**. Selected bond lengths and angles and torsion angles are as follows: C1−N1 1.347(7), N1−O1 1.353(5), O1−C25 1.467(7), C1−C2 1.439(7), C1−C6 1.431-(7) Å; C1−N1−O1 112.0(4), N1−O1−C25 111.9(4)°; O1−N1−C1−C2 −0.5(7), O1−N1−C1−C6 178.6(4), C1−N1−O1−C25 164.2(5)°.

arylaminyl to **8**, an alternate mechanism for formation of **9** proposed by us. Formation of **1**−**3** can be explained by hydrogen abstraction from **9** by arylaminyl (or *tert*-butoxyl) radical (eq 5), and formation of azobenzene **6** can be accounted for by eq 6.

X-ray Crystallographic Analysis. Recrystallization of **1a** and **3c** from MeOH gave a single-crystal suitable for X-ray crystallographic analysis. ORTEP drawings are depicted in Figures 2 and 3, together with selected bond lengths and angles and torsion angles.

In **1a**, the N and O atoms are coplanar with the benzene ring A (C1−C6) within 0.049 Å. While the benzene ring C (C13−C18) makes a dihedral angle of 41.5° for the benzene ring A, the benzene ring B (C7−C12) makes a dihedral angle of 86.0° for the benzene ring A. A very similar structure is found for **3c**. Thus, the N and O atoms are coplanar with the A benzene ring (C1−C6) within 0.047 Å, and the dihedral angles between the A and B benzene rings, between the A and C benzene rings, and between the A and D benzene rings are 89.2, 24.7, and 50.2°, respectively. It is therefore shown that both radicals have a large steric congestion around the radical center. While the unpaired electron spin can be delocalized to some extent onto the benzene ring C, it is likely that delocalization onto the benzene ring B is very small or negligible small.

Such structures are very similar to those of the corresponding sulfur analogues **10**[22] and **11**:[16] the N and S atoms are coplanar with the A benzene ring, and the dihedral angles between the A and B benzene rings and between the A and C benzene rings are 87.3 and 34.1° (**10**), and those between the A and B benzene rings, between the A and C benzene rings, and between the A and D benzene rings are 86.7, 27.3, and 49.2° (**11**), respectively.

(22) Miura, Y.; Momoki, M.; Fuchikami, T.; Teki, Y.; Itoh, K. Mizutani, H. *J. Org. Chem.* **1996**, *61*, 4300.

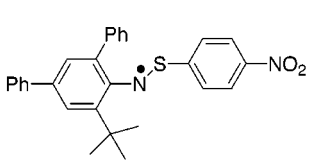

10

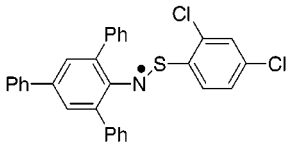

11

It is also noted that the N−O bonds [1.358(2) (**1a**) and 1.353(5) Å (**3c**)] are somewhat shorter than typical N(sp^2)−O bonds (1.397 Å). Since the N−O bonds has have the characteristics of a two-center three-electron bond in which the unpaired electron is accommodated in the antibonding orbital, the shorter bond lengths can be explained in terms of this characteristic bond nature.[23]

ESR Spectra. ESR measurements for **1**−**3** were carried out at 20 °C using benzene as the solvent. The hyperfine coupling (hfc) constants and *g* values are summarized in Table 1. As found in Figure 1, the ESR spectrum of **1a** is constituted of a broad 1:1:1 triplet (a_N = 1.01 mT, g = 2.0042) with a large peak-to-peak line width (ΔH_{pp}) of 0.31 mT. No hyperfine couplings due to aromatic protons were observed. Such a large ΔH_{pp} value can be attributable to the presence of many unresolved aromatic and aliphatic protons with small or very small hfc constants. Almost similar ESR spectra were observed for **1b**, **1c**, and **3a**−**c**. To reduce the line widths of the spectra, the phenyl groups at the 2, 4, and 6 positions of the anilino benzene ring were deuterated. The deuterated radicals **1a**-d_{10} and **3a**-d_{15} were prepared by the reaction of lithium 2,4-di(phenyl-d_5)-6-*tert*-butylphenylamide or

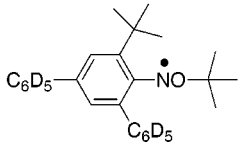

1a-d_{10}

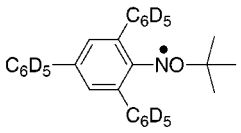

3a-d_{15}

lithium 2,4,6-tri(phenyl-d_5)phenylamide with **5** in the same manner as for the corresponding nondeuterated radicals. An ESR spectrum of **1a**-d_{10} is depicted in Figure 4, which shows a 1:1:1 triplet of 1:2:1 triplets pattern. Computer simulation of this spectrum gave a_N = 1.00 mT and a_H (2H) = 0.170 mT. The protons giving a 1:2:1 triplet splitting are assigned to the two anilino meta protons. A very similar ESR spectrum was observed for of **3a**-d_{15}, and computer simulation gave a_N = 0.999 and a_H (2H) = 0.165 mT.

In contrast to **1** and **3**, **2** showed a hyperfine splitting due to aromatic protons without deuterating the substituted benzene rings and computer simulation gave a_N = 1.05 and a_H = 0.158 mT (2 H) (g = 2.0043). This observation indicates that the line broadening observed in the ESR spectra of the nondeuterated **1** and **3** radicals can be attributed to the protons of the 4-aryl group, indicating that there is some spin delocalization onto the 4-aryl group. This is in accordance with the X-ray crystallographic results of **1a** or **3c** which shows the twisting angles of the 4-aryl groups are not large (**1a** 41.5, **3c** 24.7°).

Table 1. ESR and UV−Vis Data for 1−3, 13, and 14 in Benzene at 20 °C

radical	a_N/mT	g	λ_{max}/nm (ϵ/L mol^{-1} cm^{-1})
1a	1.01	2.0042	545 (1230), 334 (28600)
1b	0.997	2.0041	545 (1270), 334 (27200)
1c	0.999	2.0042	553 (1120), 342 (29900)
1a-d_{10} [a,b]	1.00	2.0042	
2[a,c]	1.05	2.0043	492 (1040), 368 (7680)
3a[d]	1.00	2.0041	542 (1280), 336 (28300)
3b	0.987	2.0042	540 (1190), 333 (24900)
3c	0.984	2.0043	546 (1230), 380 (950 sh), 341 (31700)
3a-d_{15} [a,e]	0.999	2.0041	
13	0.987	2.0038	
14	1.27	2.0062	
13-d_{10} [a,f]	0.990	2.0038	
14-d_{10}	1.27	2.0062	

[a] The hyperfine coupling constants are determined by computer simulation. [b] a_H for the anilino meta protons (2 H) is 0.170 mT. [c] a_H for the anilino meta protons (2 H) is 0.158 mT. [d] The ϵ values for the radical of an 92% purity. [e] a_H for the anilino meta protons (2 H) is 0.165 mT. [f] a_H for the anilino meta protons (2 H) is 0.176 mT.

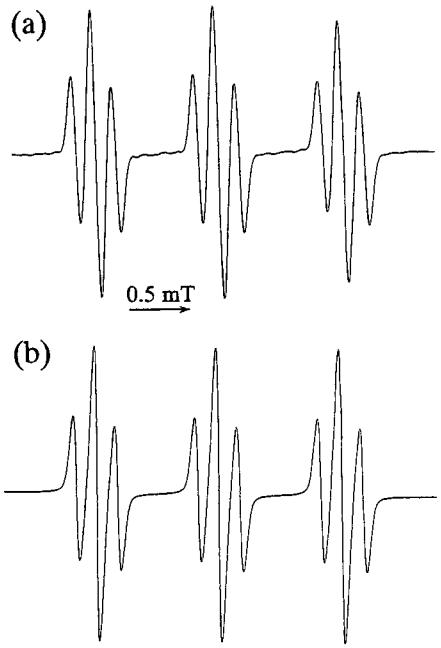

Figure 4. ESR spectrum of **1a**-d_{10} in benzene at 20 °C. (a) Observed ESR spectrum; (b) computer simulation.

It is known to be very difficult to detect satellite lines due to ^{17}O at the natural abundance because of its very low percent value of the natural abundance (0.037%). Low successful attempts to detect ^{17}O satellite lines for **1**−**3**, as had been expected, resulted in failure. On the other hand, the molecular orbital (MO) calculations for **1a** based on the density functional theory predicted 0.146 for the spin density on oxygen, as described below. This relatively high spin density on oxygen leads to high *g* values because oxygen has a large spin−orbit coupling parameter of 152 cm^{-1}. The high *g* values of **1**−**3** (2.0041−2.0043), compared with those (2.0033) of *N*-alkylarylaminyls (ArNR),[24] are therefore explained in terms of a relatively high spin density on oxygen.

The Molecular Orbital Calculations. Ab initio MO calculations based on the density functional theory were carried out for **1a**. The optimized structure was calculated by the MNDO/AM1 method, and the atomic spin density

(23) Baird, N. C. *J. Chem. Educ.* **1977**, *54*, 291.

(24) Nelsen, S. F.; Landis, R. T., II *J. Am. Chem. Soc.* **1973**, *95*, 8707.

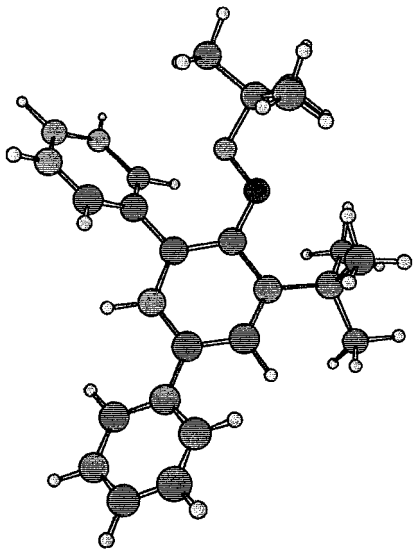

Figure 5. The optimized structure of **1a** calculated by the MNDO/AM1 method. Selected bond lengths and angles and torsion angles are as follows: C1−N1 1.372, N1−O1 1.293, O1−C23 1.485 Å; C1−N1−O1 117.0, N1−O1−C23 114.7°; O1−N1−C1−C2 −0.32, O1−N1−C1−C6 −176.7, C1−N1−O1−C23 176.5°.

calculations were performed by the UB3LYP method (basis set STO 6-31G) using Gaussian 98W.[25]

The optimized structure is depicted in Figure 5. Although there are some small deviations from the X-ray crystallographic structure, satisfactory agreements are found between them. One of the large deviations is the dihedral angle between the A and B benzene rings. While the X-ray crystallographic structure showed a dihedral angle of 86.0°, the calculations give 49.8°. On the other hand, the calculated dihedral angle (33.7°) between the A and C benzene rings is in satisfactory agreement with the X-ray results (41.5°). The calculated hfc constants are shown in Table 2, together with the ESR results. Although the calculations give higher values than the ESR results, the deviations are small. It is therefore concluded that the calculations provide reliable results. Figure 6 shows the calculated spin density distribution of **1a**, which reveals that the high spin density positions are the nitrogen, oxygen, and anilino benzene ring. Figure 6 also shows that, although there are some spin densities on the 4-phenyl group (C benzene ring), there is little or no spin densities on the 2-phenyl group (B benzene ring), in accordance with the ESR and X-ray crystallographic results.

UV−Vis Spectra of Radicals. The UV−Vis spectra of **1**−**3** were measured using benzene as the solvent. A typical spectrum of **1a** is depicted in Figure 7, and the UV−Vis spectral data are summarized in Table 1. As

(25) Gaussian 98, Revision A.9, Frisch, M. J.; Trucks, G. W.; Schlegel, H. B.; Scuseria, G. E.; Robb, M. A.; Cheeseman, J. R.; Zakrzewski, V. G.; Montgomery, J. A., Jr.; Stratmann, R. E.; Burant, J. C.; Dapprich, S.; Millam, J. M.; Daniels, A. D.; Kudin, K. N.; Strain, M. C.; Farkas, O.; Tomasi, J.; Barone, V.; Cossi, M.; Cammi, R.; Mennucci, B.; Pomelli, C.; Adamo, C.; Clifford, S.; Ochterski, J.; Petersson, G. A.; Ayala, P. Y.; Cui, Q.; Morokuma, K.; Malick, D. K.; Rabuck, A. D.; Raghavachari, K.; Foresman, J. B.; Cioslowski, J.; Ortiz, J. V.; Baboul, A. G.; Stefanov, B. B.; Liu, G.; Liashenko, A.; Piskorz, P.; Komaromi, I.; Gomperts, R.; Martin, R. L.; Fox, D. J.; Keith, T.; Al-Laham, M. A.; Peng, C. Y.; Nanayakkara, A.; Challacombe, M.; Gill, P. M. W.; Johnson, B.; Chen, W.; Wong, M. W.; Andres, J. L.; Gonzalez, C.; Head-Gordon, M.; Replogle, E. S.; Pople, J. A.; Gaussian, Inc., Pittsburgh, PA, 1998.

Table 2. Calculated Hyperfine Coupling Constants for 1a

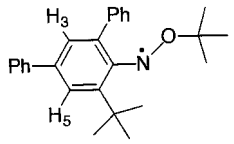

posn	calcd hfc const[a,b]	obsd hfc const[b,c]
N	1.338	1.00
O	−1.097	
H_3	0.313	0.170
H_5	0.301	0.170

[a] The hfc constants are given in mT. [b] The hfc constants are calculated by the UB3LYP method (basis set STO 6-31G). [c] The hfc constants for **1a**-d_{10} are shown in the absolute values.

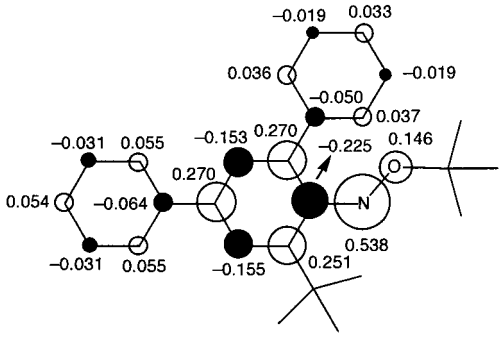

Figure 6. The total atomic spin densities for **1a** calculated based on the density functional theory (UB3LYP method/STO 6-31G basis set).

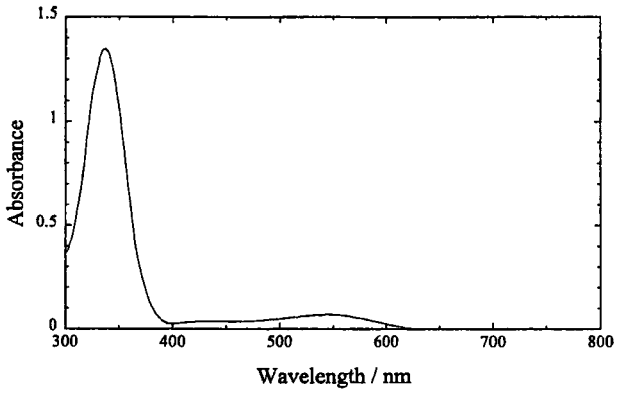

Figure 7. UV−Vis spectrum of a solution of 4.68×10^{-5} M of **1a** in benzene.

found in Figure 7, a strong absorption due to the $\pi-\pi^*$ transition is observed at 334 nm, and in the visible region a weak absorption with ϵ of 1230 is observed at 545 nm. The absorption in the visible region is corresponding to the characteristic red color of radical. While **1b**, **1c**, and **3a**−**c** showed a very similar UV−Vis spectrum to that of **1a**, that of **2** was considerably different from them. This is due to the narrowed π-conjugated system of **2** caused by replacement of a phenyl group by a *tert*-butyl group.

Generation of Persistent *N*-Alkoxyarylaminyl Radicals by Addition of Alkyl Radicals to Nitrosobenzenes. An alternate useful method for generation of *N*-alkoxyarylaminyl radicals is an addition of alkyl radicals to nitrosobenzenes. This method is well-known as the spin trapping technique, which is useful as a convenient method to identify transient free radicals.[26] When nitrosobenzene is used as the spin trapping agent for trapping of alkyl radicals, the formed spin adducts

Scheme 3

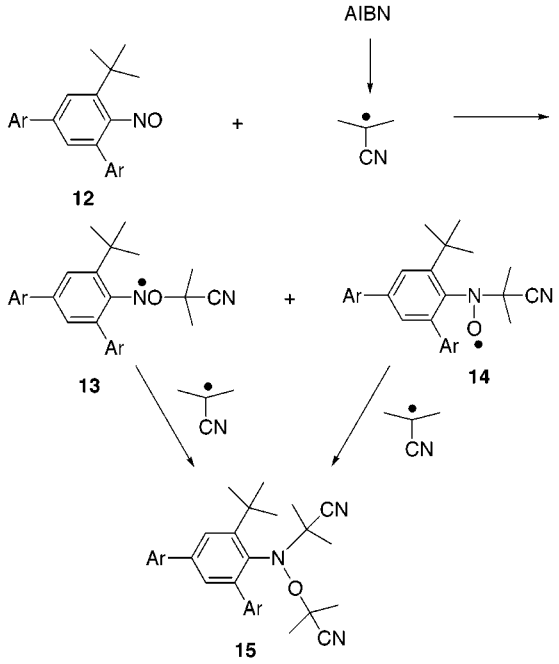

12–15: Ar = Ph
12-d_{10}–**14**-d_{10}: Ar = C_6D_5

are *N*-alkylarylaminoxyls. However, when sterically congested 2,4,6-tri-*tert*-butylnitrosobenzene is used as the spin trapping agent and trapped radicals are *tert*-alkyl radicals, *N*-alkoxyarylaminyls are exclusively formed as the spin adducts.[8] Using this method, we prepared *N*-alkoxyarylaminyls **13** (Scheme 3). A solution of 2,4-diphenyl-6-*tert*-butylnitrosobenzene (**12**) and 0.65 equiv of azobisisobutyronitrile (AIBN) in benzene was heated at 70 °C for 1 h, and ESR signals from the solution were measured. The ESR spectra obtained showed that there were two kinds of radicals, *N*-alkoxyarylaminyl **13** (a_N = 0.987 mT, g = 2.0038) and arylaminoxyl **14** (a_N = 1.27 mT, g = 2.0062) in an intensity ratio of 1:3. When a deuterated nitrosobenzene, 2,4-di(phenyl-d_5)-6-*tert*-butylnitrosobenzene (**12**-d_{10}), was used, the spectrum of **13**-d_{10} showed additional hyperfine splittings due to the anilino meta protons, and computer simulation gave a_N = 0.990 and a_H (2H) = 0.176 mT (g = 2.0038). On the other hand, the ESR spectrum of **14**-d_{10} showed no change other than narrowing of the line-width. As found in Table 1, the a and g values for **13** and **13**-d_{10} are similar to those of **1**−**3**, while the a_N's (1.27 mT) for **14** and **14**-d_{10} are similar to those of 2,6-disubstituted *N*-*tert*-alkylarylaminoxyls **16** and **17** (a_N = 1.322−1.338 mT).[27]

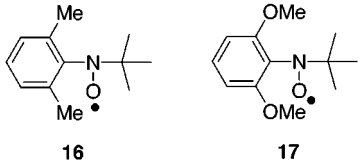

16 **17**

Isolation of **13** from the reaction mixture was tried. A mixture of **12** and AIBN (0.65 equiv) was heated at the reflux temperature for 1 h, and the resulting mixture was chromatographed to give **13** as a red oil in 3.9% yield. Although the spin concentration of the oil determined by ESR was very high (89%), the oil never solidified even upon cooling to low temperatures. When an excess (1.5 equiv) of AIBN was employed in the reaction with **12**, nonspin product **15** was obtained in 27% yield. When a benzene solution of **15** in an ESR tube was directly heated to 70 °C in the cavity of an ESR instrument, only an ESR signal due to **14** was observed, indicating that the C−O bond cleavage exclusively occurs in thermolysis of **15** at 70 °C.

Table 3. Results of Magnetic Measurements for 1 and 3

radical	Curie const/emu K mol^{-1} (radical purity/%[a])	θ/K
1a	0.369 (98)	−0.45
1b	0.375 (100)	−1.5
1c	0.365 (97)	0.3
3c	0.366 (98)	−0.3

[a] The radical purities are caluculated based on the Curie constant of 0.375 emu K mol^{-1} for the pure radicals.

Thermal Stability. To evaluate the thermal stability of **1**−**3**, benzene solutions of **1a**, **2**, and **3a** were heated in a degassed Pyrex glass tube at 80 °C for 10 days. After heating, the radical concentrations of the resulting solutions were determined by ESR or UV−Vis spectra. Surprisingly, even after heating at 80 °C for 10 days, the radical concentrations were kept more than 80%, and no rearrangement of *N*-alkoxyarylaminyls to the corresponding aminoxyls took place during heating. On the basis of the above results, we conclude that the present *N*-alkoxyarylaminyls are thermally very stable. Previously, it was reported that *N*-*tert*-butoxy-2,6-diphenyl-4-*tert*-butylphenylaminyl (**18**) rearranged to the corresponding aminoxyls at room temperature.[10] Since **18** is structurally very similar to **2**, we are interested in this difference. One possible explanation for the rearrangement of **18** is influences of impurities. While the radicals used in our experiment are pure, the observed rearrangement occurs in a solution containing many impurities. Further experiments to clarify this point will be required.

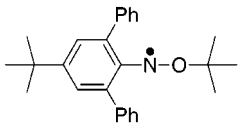

18

Magnetic Properties of Isolated Radicals. The magnetic properties of the isolated five radicals were measured on a SQUID magnetometer using polycrystalline samples in the temperature range 1.8−300 K. The diamagnetic contributions were estimated using Pascal's constants.

The results are summarized in Table 3. The purities of the isolated radicals calculated based on the Curie constant of 0.375 emu K mol^{-1} for the radicals of the 100% purity were 97−100%.

The $\chi_{mol}T$ vs T plots for **1c** are shown in Figure 8. The $\chi_{mol}T$ value is constant in the temperature range 20−300 K, and below 20 K it increases slightly. This magnetic behavior indicates that the radical molecules weakly couple ferromagnetically. The θ value determined using the Curie−Weiss law was 0.3 K. On the other hand, radicals **1a**, **1b**, and **3c** showed weak antiferromagnetic

(26) Janzen, E. G. *Acc. Chem. Res.* **1971**, *4*, 31,
(27) (a) Calder, A.; Forrester, A. R. *Chem. Commun.* **1967**, 682. (b) Hoffmann, A. K.; Feldman, A. M.; Gelblum, E. *J. Am. Chem. Soc.* **1964**, *86*, 646.

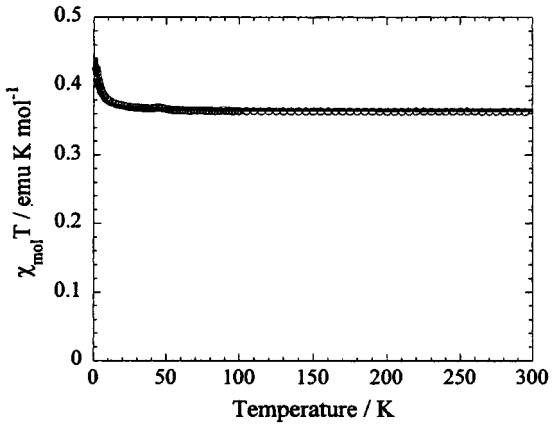

Figure 8. $\chi_{mol}T$ vs T plots for **1c**. The solid curve represents the theoretical line calculated using the Curie−Weiss law (θ = 0.30 K).

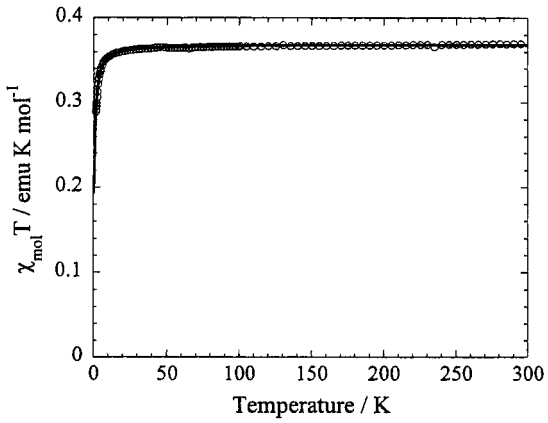

Figure 9. $\chi_{mol}T$ vs T plots for **1a**. The solid curve represents the theoretical line calculated using the Curie−Weiss law (θ = −0.45 K).

interactions. The $\chi_{mol}T$ vs T plots for **1a** are shown in Figure 9. The $\chi_{mol}T$ value is constant in the temperature range 20−300 K, and below 20 K, it slightly decreases. Using the Curie−Weiss law θ was determined to be −0.45 K.

The weak magnetic interactions of **1a** can be explained by the crystal structure depicted in Figure 10. Radical molecules are stacked along the *a* axis, and the shortest intermolecular distance between the neighboring radical molecules is found for O−C2′, which is 4.68 Å. This distance is too long to induce a strong magnetic interaction. As found in Figure 10, the presence of bulky *tert*-butyl groups prevents the neighboring radical molecules from approaching, which makes the intermolecular interaction weak. This is in contrast to thioaminyl radicals which show strong interactions.[13] Since the signs of the spin densities at those sites are opposite, the McConnell mechanism predicts that the interaction is antiferromagnetic, which is in accordance with the experimental results.

Conclusions

Thermally very stable *N*-*tert*-butoxylarylaminyls **1**−**3** were prepared and isolated as radical crystals. X-ray crystallographic analyses of the isolated radicals showed that N and O are coplanar with the anilino benzene ring. The MO calculations based on the density functional

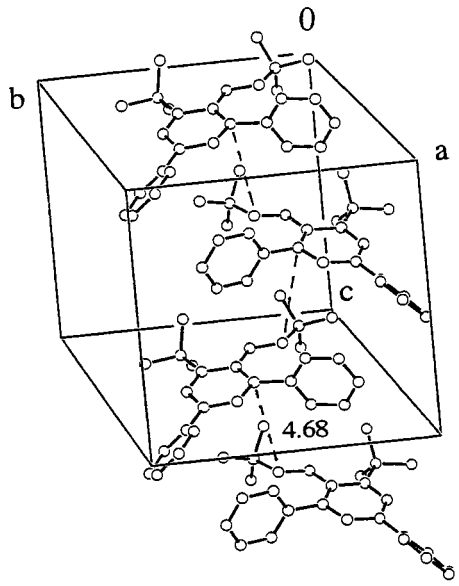

Figure 10. Crystal structure of **1a**. The hydrogen atoms are omitted for clarity.

theory predicted that the unpaired electron spin is widely delocalized over the N, O, and the anilino benzene ring, in accordance with the ESR and X-ray crystallographic results. The magnetic susceptibility measurements showed that one radical showed a weak ferromagnetic interaction, and three radicals weak antiferromagnetic interactions. The weak magnetic interactions were attributed to the presence of bulky *tert*-butyl groups.

Experimental Section

IR, UV−Vis, and ^{1}H NMR measurements were carried out as previously reported.[1] ESR spectra were recorded with a Bruker ESP300 spectrometer. Field calibration was carried out with Fremy's salt in aqueous dilute K_2CO_3 (a_N = 13.09; g = 2.0055). Magnetic susceptibility measurements were performed with a Quantum Design MPMS2 SQUID magnetometer using polycrystalline samples in the temperature range 1.8−300 K. The diamagnetic components were estimated by Pascal's sum rule.

Materials. 2,4-diphenyl-6-*tert*-butylaniline, 2,4-bis(4-fluorophenyl)-6-*tert*-butylaniline, 2,4-bis(4-chlorophenyl)-6-*tert*-butylaniline, 2,6-bis(4-chlorophenyl)-4-*tert*-butylaniline, 2,4,6-tris(4-fluorophenyl)aniline, 2,4,6-tris(4-chlorophenyl)aniline, 2,4-di(phenyl-d_5)-6-*tert*-butylaniline, and 2,4,6-tri(phenyl-d_5)-aniline were prepared by the Pd-catalyzed cross−coupling reaction of the corresponding bromoanilines with arylboronic acids using the usual procedure.[28] *tert*-Butyl peroxybenzoate (**5**) was commercially available and used without purification. Column chromatography was conducted on Silica gel [Kanto Chemical Co. Inc. silica gel 60N (63−210 μm)] or alumina (Merck Aluminum oxide 90).

2,4-Diphenyl-6-*tert*-butylnitrosobenzene (12). To a stirred solution of 0.94 g (3.1 mmol) of 2,4-diphenyl-6-*tert*-butylaniline in 16 mL of dichloromethane cooled in an ice−water bath was added dropwise a solution of 1.35 g of *m*-chloroperoxybenzoic acid (70%) in 30 mL of dichloromethane for 15 min, and the resulting mixture was stirred for 30 min at 0 °C. After water (20 mL) was added, the dichloromethane solution was separated, washed with $NaHCO_3$, and brine, and dried over $MgSO_4$. After filtration and evaporation, the residue (oil) was column chromatographed on silica gel with 1:1 hexane−benzene to give **12** as a green oil in 72% yield. ^{1}H NMR ($CDCl_3$) δ 1.72 (s, 9 H), 6.83 (d, J = 7.3 Hz, 2 H), 7.20 (d, J = 2.0 Hz, 1H), 7.29−

(28) Miura, Y.; Oka, H.; Momoki, M. *Synthesis* **1995**, 1419.

7.45 (m, 6 H), 7.63 (d, J = 7.3 Hz, 2 H), 7.87 (d, J = 2.0 Hz, 1H); HRMS (FAB) calcd for $C_{22}H_{21}NO$ 315.1623, found 315.1632.

2,4-Di(phenyl-d_5)-6-*tert*-butylnitrosobenzene (12-d_{10}). This compound was prepared by the same procedure as that for **12**. Green oil; yield 70%; ^{1}H NMR ($CDCl_3$) δ 1.72 (s, 9 H), 7.20 (d, J = 2.0 Hz, 1H), 7.87 (d, J = 2.0 Hz, 1H); HRMS (FAB) calcd for $C_{22}H_{11}D_{10}NO$ 325.2241, found 325.2238.

General Procedure for Preparation of Radicals. A solution of 5.80 mmol of an aniline in 100 mL of anhyrous THF was cooled to −78 °C, and 4.0 mL of a butyllithium hexane solution (1.6 M) was added with stirring. A solution of 2.48 g (12.8 mmol) of *tert*-butyl peroxybenzoate in 5 mL of anhydrous THF was then added dropwise to the solution at −78 °C, and the resulting red solution was stirred for 1.5 h at the same temperature and then warmed slowly to room temperature. The reaction mixture was extracted with benzene, and the benzene solution was washed with an aq 10% $Na_2S_2O_3$ solution and then brine, and dried over $MgSO_4$. After filtration and evaporation, the residue was column chromatographed on silica gel with 1:3 benzene−hexane (**1a**−**c**, **2**, **3b**, and **3c**) or 1:4 benzene−hexane (**3a**), and evaporation of the solvent gave a red radical mass (**1a**−**c**, **2**, **3b**, and **3c**) or an oil (**3a**). The solid masses were then recrystallized from MeOH (**1a**−**c**, **2**, and **1a**-d_{10}) or MeOH-ethyl acetate (**3b** and **3c**).

***N*-*tert*-Butoxy-2,4-diphenyl-6-*tert*-butylphenylaminyl (1a):** red plates; mp 114.5−116 °C; yield 24%. Anal. Calcd for $C_{26}H_{30}NO$: C, 83.83; H, 8.12; N, 3.76. Found: C, 83.49; H, 8.12; N, 3.69.

***N*-*tert*-Butoxy-2,4-bis(4-fluorophenyl)-6-*tert*-butylphenylaminyl (1b):** red needles; mp 111−113 °C; yield 20%. Anal. Calcd for $C_{26}H_{28}F_2NO$: C, 76.44; H, 6.91; N, 3.43; F, 9.30. Found: C, 76.31; H, 6.88; N, 3.32; F, 9.17.

***N*-*tert*-Butoxy-2,4-bis(4-chlorophenyl)-6-*tert*-butylphenylaminyl (1c):** red needles; mp 137−139 °C; yield 17%. Anal. Calcd for $C_{26}H_{28}Cl_2NO$: C, 70.75; H, 6.39; N, 3.17. Found: C, 70.74; H, 6.45; N, 3.22.

***N*-*tert*-Butoxy-2,4-di(phenyl-d_5)-6-*tert*-butylphenylaminyl (1a-d_{10}):** red plates; mp 114−115.5 °C; yield 25%. Anal. Calcd for $C_{26}H_{20}D_{10}NO$: C, 81.62; H, 5.27; N, 3.66; O, 4.18. Found: C, 81.70; H, 5.33; N, 3.54; O, 4.29.

***N*-*tert*-Butoxy-2,6-bis(4-chlorophenyl)-4-*tert*-butylphenylaminyl (2):** red needles; mp 169−170 °C; yield 20%. Anal. Calcd for $C_{26}H_{28}Cl_2NO$: C, 70.75; H, 6.39; Cl, 16.06; N, 3.17; O, 3.62. Found: C, 70.47; H, 6.19; Cl, 16.10; N, 3.24; O, 3.74.

***N*-*tert*-Butoxy-2,4,6-triphenylphenylaminyl (3a):** red oil; yield 18%; HRMS (FAB) calcd for ($C_{28}H_{26}NO$ + H) 393.2093, found 393.2074. The spin concentration of of this radical determined by ESR was 92%.

***N*-*tert*-Butoxy-2,4,6-tris(4-fluorophenyl)phenylaminyl (3b):** red needles; mp 136−137 °C; yield 17%. Anal. Calcd for $C_{28}H_{23}F_3NO$: C, 75.32; H, 5.19; N, 3.14; F, 12.77. Found: C, 75.12; H, 5.11; N, 3.18; F, 12.75.

***N*-*tert*-Butoxy-2,4,6-tris(4-chlorophenyl)phenylaminyl (3c):** red needles; mp 152−154 °C; yield 18%. Anal. Calcd for $C_{28}H_{23}Cl_3NO$: C, 67.82; H, 4.68; Cl, 21.45; N, 2.82; O, 3.23. Found: C, 67.62; H, 4.91; Cl, 21.69; N, 2.85; O, 3.59.

2,2′,4,4′-Tetraphenyl-6,6′-di-*tert*-butylazobenzene (6): red fine plates, 112−113 °C (from MeOH); yield 0.76%; ^{1}H NMR ($CDCl_3$) δ 1.24 (s, 18 H), 7.18−7.63 (m, 24 H). Calcd for $C_{44}H_{42}N_2$: C, 88.25; H, 7.07; N, 4.68. Found: C, 88.02; H, 7.26; N, 4.73.

Preparation and Isolation of *N*-[(2-Cyano-2-propoxy)-2,4-diphenyl-6-*tert*-butylphenylaminyl (13). A solution of 250 mg (0.80 mmol) of **12** and 85 mg (0.52 mmol) of azobisisobutyronitrile (AIBN) in 30 mL of benzene was refluxed for 1 h. After cooling to room temperature, the benzene was evaporated, and the residue was column chromatographed on silica gel with 1:1 benzene−hexane to give **13** as a red oil in 3.9% yield. The spin concentration of **13** determined by ESR was 89%.

***N*-(2-Cyano-2-propoxy)-*N*-(2-cyano-2-propyl)-2,4-diphenyl-6-*tert*-butylaniline (15).** A solution of 250 mg (0.80 mmol) of **12** and 197 mg (1.20 mmol) of AIBN in 30 mL of benzene was refluxed for 20 h under nitrogen. After the solvent was evaporated under reduced pressure, the residue was chromatographed on alumina with benzene as eluant, and recrystallization from MeOH gave **15** in 27% yield. Mp 95 °C (decomp); IR (KBr) 2220 cm^{-1} (CN); ^{1}H NMR ($CDCl_3$) δ 1.29 (s, 3H), 1.58 (s, 3H), 1.61 (s, 3 H), 1.71 (s, 9H), 1.77 (s, 3 H), 7.13 (d, J = 2.4 Hz, 1 H), 7.29−7.58 (m, 10 H), 7.81 (d, J = 2.4 Hz, 1 H). Anal. Calcd for $C_{30}H_{33}N_3O$: C, 79.79; H, 7.37; N, 9.30. Found: C, 79.49; H, H, 7.48; N, 9.28.

ESR Measurements of a Solution of 12 and AIBN in Benzene at 70 °C. A degassed benzene solution (1.0 mL) of **12** (8.0 mM) and AIBN (5.2 mM) in an ESR tube was put in the cavity of an ESR instrument, and ESR spectra from the solution were measured at 70 °C.

ESR Measurements of a Benzene Solution of 15 at 70 °C. A degassed benzene solution (1.0 mL) of **15** (4.4 mM) in an ESR tube was put in the cavity of an ESR instrument, and ESR spectra from the solution were measured at 70 °C.

X-ray Crystallographic Analysis of 1a.[29] A red plate crystal of $C_{26}H_{30}NO$ (372.53) having approximate dimensions of 0.80 × 0.40 × 0.20 mm was mounted on a glass fiber. All measurements were made on a Rigaku RAXIS−RAPID Imaging Plate diffractometer with graphite monochromated Mo−Kα radiation (λ = 0.71069 Å): orthorhombic space group *P*bca (No. 61), a = 36.9243(9), b = 11.2495(3), c = 10.9599(3) Å, V = 4552.5(2) Å^3, Z = 8, D_c = 1.087 g cm^{-3}. The data were collected at 23 ± 1 °C to a maximum 2θ value of 55.0°. A total of 110 images, corresponding to 220.0° oscillation angles, were collected with 2 different goniometer settings. Exposure time was 1.70 min per degree. The camera radius was 127.40 mm. Readout was performed in the 0.150 mm pixel mode. Data were processed by the PROCESS-AUTO program package. Of 13507 reflections measured 5112 were unique (R_{ini} = 0.017), 2310 of which were considered as observed ($I > 3.00\sigma(I)$).

The structure was solved by direct methods and expanded using Fourier techniques.[30] The non-hydrogen atoms were refined anisotropically. Hydrogen atoms were placed in the fixed position and not refined. The final cycle of full matrix least-squares refinement was based on 2310 observed reflections and 253 variable parameters and converged with unweighted and weighted agreement factors of R = 0.078 and R_w = 0.116. GOF = 1.57.

X-ray Crystallographic Analysis of 3c.[29] A red plate crystal of $C_{28}H_{23}Cl_3NO$ (495.85) having approximate dimensions of 0.08 × 0.07 × 0.40 mm was mounted on a glass fiber. All measurements were made on a Rigaku RAXIS−RAPID Imaging Plate diffractometer with graphite monochromated Mo−Kα radiation (λ = 0.71069 Å): monoclinic space group $P2_1/n$ (No. 14), a = 24.8127(1), b = 17.0245(3), c = 5.9797(1) β = 96.9111(3)°, V = 2507.62(8) Å^3, Z = 4, D_c = 1.313 g cm^{-3}. The camera radius was 127.40 mm. Readout was performed in the 0.100 mm pixel mode. Data were processed by the PROCESS-AUTO program package. Of 17060 reflections measured 5499 were unique (R_{ini} = 0.048), 2518 of which were considered as observed ($I > 3.00\sigma(I)$).

The structure was solved by direct methods and expanded using Fourier techniques.[30] The non-hydrogen atoms were refined anisotropically. Hydrogen atoms were placed in the fixed position and not refined. The final cycle of full matrix least-squares refinement was based on 2518 observed reflections and 298 variable parameters and converged with unweighted and weighted agreement factors of R = 0.095 and R_w = 0.164. GOF = 1.87.

Supporting Information Available: Tables of X-ray crystallographic data for compounds **1a** and **3c**. This material is available free of charge via the Internet at http://pubs.acs.org.

JO0106288

(29) The crystallographic computing was done by the TEXSAN structure analysis software.

(30) SIR92: Altomare, A.; Burla, M. C.; Camalli, M.; Cascarano, M.; Giacovazzo, C.; Guagliardi, A.; Polidori, G. *J. Appl. Crystallogr.* **1994**, *27*, 435.